Si nanostructures fabricated by anodic oxidation with an atomic force microscope and etching with an electron cyclotron resonance source

E. S. Snow[a)]
Naval Research Laboratory, Washington, DC 20375

W. H. Juan and S. W. Pang
Solid State Electronics Laboratory, Department of Electrical Engineering and Computer Science, The University of Michigan, Ann Arbor, Michigan 48109-2122

P. M. Campbell
Naval Research Laboratory, Washington, DC 20375

(Received 14 November 1994; accepted for publication 3 February 1995)

Nanometer-scale Si structures have been fabricated by anodic oxidation with an atomic force microscope (AFM) and dry etching using an electron cyclotron resonance (ECR) source. The AFM is used to anodically oxidize a thin surface layer on a H-passivated (100) Si surface. This oxide is used as a mask for etching in a Cl_2 plasma generated by the ECR source. An etch selectivity >20 was obtained by adding 20% O_2 to the Cl_2 plasma. The AFM-defined mask withstands a 70 nm deep etch, and linewidths$\sim$10 nm have been obtained with a 30 nm etch depth. © *1995 American Institute of Physics.*

The scaling of device dimensions down to the nanometer range has created a demand for novel fabrication techniques with increased resolution capabilities. Typically, pattern definition for nanometer scale features is accomplished by high energy electron-beam exposure of a polymer resist. This technique has limited resolution capabilities typically in the range of 20–30 nm. More recently, proximal probes such as the scanning tunneling microscope (STM) and the atomic force microscope (AFM) have attracted attention as potential new tools for nanofabrication because of their demonstrated ability to image and manipulate matter at the atomic level.[1] The challenge for this new technology is to translate this ultimate level of control into actual device fabrication.

One promising approach is based on tip-induced oxidation of a sample surface[2] followed by pattern transfer via selective etching.[3] This process has been successful because of the reliability of the exposure process and the robustness of the surface oxide to certain very selective liquid etches. This oxidation and selective etching process has been used to fabricate working Si device structures,[4] including a 0.1 μm gate-length Si metal–oxide–semiconductor field effect transistor.[5] In addition, an UHV-based exposure technique has demonstrated true nanometer control of the oxidation process.[6] While this UHV process demonstrates the potential resolution of the approach, continued improvement in the size of etched features is going to require directional dry etching techniques which can improve the limited aspect ratios obtained by liquid etching.

In this work, an electron cyclotron resonance (ECR) source is used to etch Si nanostructures which are patterned by selective oxidation of a H-passivated Si surface with an anodically biased AFM tip. The oxide patterns were etched in a Cl_2 plasma generated by an ECR source. ECR offers many advantages over conventional reactive ion etching (RIE). With the combination of magnetic confinement and the coupling of microwave power, the ECR source provides a dissociation efficiency that is typically more than an order of magnitude higher than RIE. This high efficiency allows the plasma to be maintained at much lower pressure than with RIE which reduces scattering of reactive species and promotes vertical etch profiles and smooth surface morphology. The independent control of ion energy by the rf-powered stage and ion flux by the microwave power provides the flexibility needed to optimize the Si etching with high etch selectivity to Si oxide. High etch selectivity is especially important in this work due to the thin ($\sim$2–4 nm) oxide mass generated by the AFM.

Using the ECR source, the etch conditions were optimized to provide high selectivity over the oxide mask, a vertical etch profile, and smooth morphology. Si nanostructures with $\sim$10 nm width and 30 nm depth were etched in a Cl_2/O_2 plasma. Wider structures with a thicker oxide were etched to a depth of 70 nm with no signs of mask degradation.

The samples for this study were cleaved from a 0.01 Ω cm (100) *n*-type Si wafer. The samples were prepared for exposure by cleaning in solvents, exposure to UV ozone, and H passivation in a 10% aqueous HF solution. After passivation the samples were mounted in an air-operated AFM. The AFM tip was a standard Si_3N_4 pyramidal tip which was coated with 30 nm of Ti from an electron-beam evaporator.

The oxide patterns were formed by exposing the H-passivated surface to an AFM tip biased in the range -4 to -7 V.[7] The exposure rate varied from 1 to 10 μm/s. High voltages and slow write speeds were used to produce thick (and wide) oxide patterns. The opposite is true for fine patterns. Since the exposure process is humidity dependent, the ambient atmosphere was maintained at $\sim$50% relative humidity during exposure.

The plasma etching system with an ECR source and a rf-powered electrode has been previously described.[8] Microwave power at 2.45 GHz is coupled into the ECR cavity by

[a)]Electronic mail: snow@bloch.nrl.navy.mil

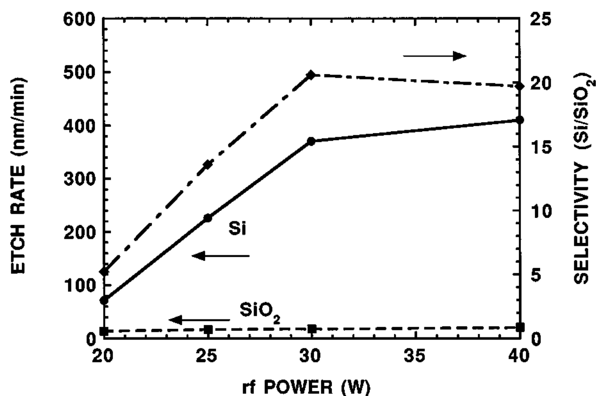

FIG. 1. Si and SiO_2 etch rates and Si/SiO_2 etch selectivity as a function of rf power. The samples were etched using 50 W microwave power at 1 mTorr. The Cl_2 and O_2 flow rates were 8 and 2 sccm, respectively.

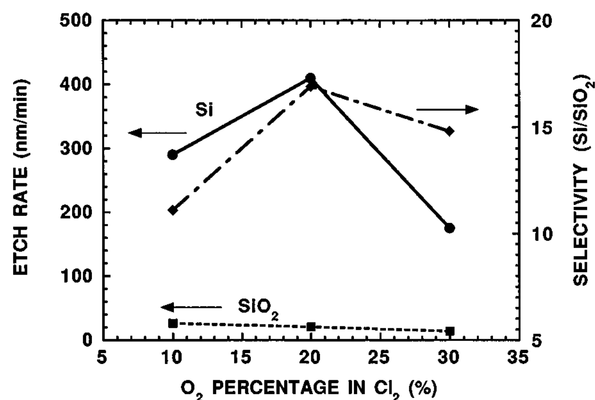

FIG. 2. The effect of O_2 on Si and SiO_2 etch rates and on Si/SiO_2 etch selectivity. The plasma was excited at 50 W microwave power, 40 W rf power at 1 mTorr and 10 sccm total gas flow.

a tunable input probe. The magnetic field for the ECR excitation is provided by 12 permanent magnets, which are spaced around a quartz disk. The sample stage is connected to a 13.56 MHz rf power supply. A self-induced dc bias voltage V_{dc} is developed between the plasma and the stage and can be used to control the ion energy. Chamber pressure is controlled by a throttle valve and a 1500 *l*/s turbomolecular pump. The gas flow rate is adjusted by a mass flow controller. Cl_2 is introduced into the chamber through a gas ring around the substrate stage, and O_2 is flowed through a separate gas ring at the bottom of the quartz disk. The stage position is fixed at 8 cm below the ECR source, and the stage temperature is set at 25 °C. Optimal etch conditions for pattern transfer were obtained by adjusting the rf power to the stage and the Cl_2 to O_2 ratio. The Si etch rate was measured by surface profilometry, and the SiO_2 rate was measured using ellipsometry on thermal oxide before and after etching. Scanning electron microscopy (SEM) and AFM were used to determine the depth and profile of the etched Si nanostructures.

In order to provide high selectivity, it is desirable to use a high density plasma with low ion energy. Since rf power determines V_{dc} and, thus ion energy, the dependence of the Si/SiO_2 selectivity on rf power was investigated. The results are shown in Fig. 1. The samples were etched with a Cl_2/O_2 plasma flowed at 8 and 2 sccm, respectively and 50 W microwave power at 1 mTorr. The Si etch rate increased from 71 to 410 nm/min while the oxide etch rate increased from 14 to 21 nm/min as the rf power increased from 20 to 40 W. The Si/SiO_2 selectivity increased initially from 5 to 21 as rf power increased from 20 to 30 W, then decreased slightly to 20 at 40 W rf power. The increase in selectivity is attributed to the relative increase of the Si to SiO_2 etch rate with rf power compared to the SiO_2 etch rate.

In addition to rf power, etch selectivity can also be improved by adding O_2 to the Cl_2 plasma.[9,10] The influence of O_2 on the Si and SiO_2 etch rates, as well as the etch selectivity is shown in Fig. 2. The plasma was excited with 50 W microwave power and 40 W rf power at 1 mTorr with 10 sccm total gas flow. The SiO_2 etch rate decreased from 26 to 14 nm/min as O_2 composition increased from 10% to 30%. The reduced oxide etch rate could be related to a decreased C concentration or to a surface which is modified by oxygen species when O_2 is added. On the other hand, the Si etch rate increased from 290 to 410 nm/min, then decreased to 175 nm/min over the same range of O_2 percentage variation. The initial increase in Si etch rate may be due to enhanced dissociation of Cl_2 in the presence of O_2. The decreasing Si etch rate at high O_2 concentration is due to a dilution effect.[11] The selectivity is thus the highest with 20% O_2.

The AFM-defined oxide patterns were etched using the

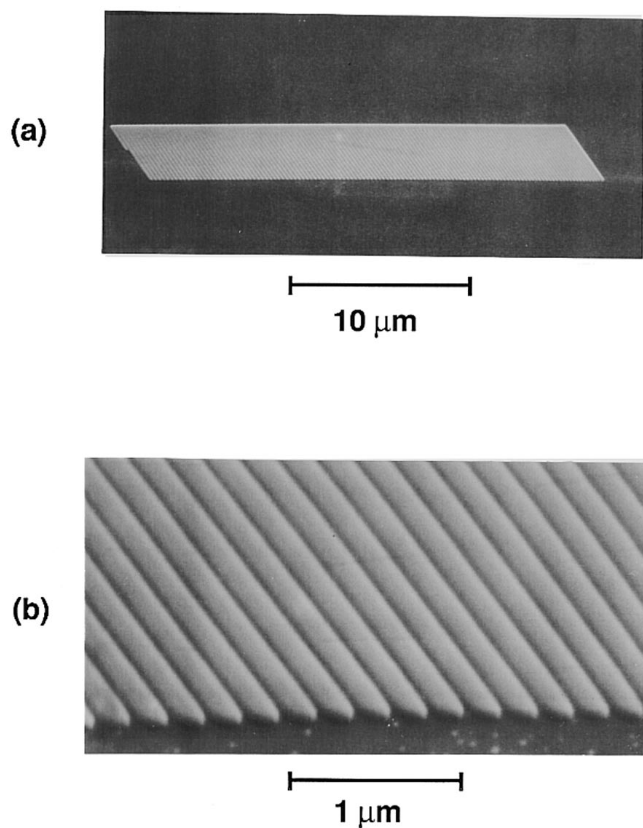

FIG. 3. (a) Low and (b) high resolution SEM images of a Si grating formed by AFM oxidation and etching with the ECR source. The linewidth is ~150 nm and the etch depth is 70 nm. The pattern was exposed at −7 V tip bias at a rate of 1 μm/s. The pattern was etched using 50 W microwave power and 30 W rf power at 1 mTorr. The Cl_2 and O_2 flow rates were 8 and 2 sccm, respectively.

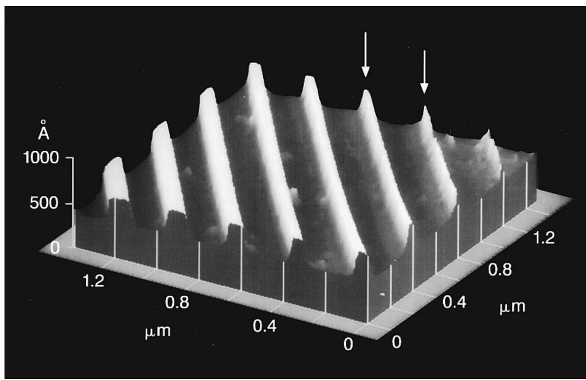

FIG. 4. AFM image of dry-etched Si wires of varying linewidth. The etch depth was 30 nm. The two lines indicated in the figure have AFM-measured linewidths of 25–30 nm and 35–40 nm, respectively. The actual linewidths are ~20 nm less than these measured values due to the finite size of the AFM tip.

Cl_2O_2 plasma generated with 50 W microwave power and 30 W rf power at 1 mTorr. Figure 3(a) shows a SEM image of a 5 μm×30 μm grating which was etched to a depth of 70 nm. The image shows that the etch has not penetrated the oxide mask. Measurements on a thermal oxide sample indicate that 4.7 nm of oxide was removed during the etch. The AFM-generated oxide is estimated to be in the range of 3–4 nm thick. The fact that the mask has withstood an etch, which removes 4.7 nm of thermal oxide, may indicate that the AFM-generated oxide contains contaminates such as C which increase the selectivity. Higher resolution imaging of the same grating [Fig. 3(b)] indicates vertical sidewalls and a smooth surface morphology.

Much finer wires are easily fabricated by this process. Figure 4 shows an AFM image of a set of etched lines with varying width. AFM line profiles indicate an etch depth of 30 nm. These profiles were also used to determine the full-width-at-half-maximum linewidth for the two lines indicated in Fig. 4. The width of the narrower of the two lines varies from 25 to 30 nm while the wider line has a measured linewidth of 35–40 nm. This measurement is clearly an overestimate of the actual linewidth due to the finite size of the AFM tip. The tip used for this image was a Si ultralever from Park Scientific Instruments which has a 20 nm tip diameter and a 3 to 1 aspect ratio. Subtracting 20 nm from the measured linewidths yields 10 nm or less for the finest lines.[12]

In conclusion, dry etching of nanometer-scale features in Si was performed using an AFM-patterned oxide as an etch mask. The AFM was used to produce oxide patterns 2–4 nm deep with linewidths down to ~10 nm. Etching with the ECR source provides high selectivity, excellent linewidth control, vertical profile, and smooth surface morphology. Features with ~10 nm width were etched 30 nm deep by the optimized conditions for minimum oxide removal. The above results clearly demonstrate that AFM anodic oxidation and dry etching with an ECR source is an effective means of producing nanometer-scale features in Si. Combining such a directional etch technique with an UHV exposure process[6] should result in true nanometer-scale control of Si processing. In addition, STM-patterned Si on GaAs has been used as a method for fabricating GaAs nanostructures.[3] Thus, true nanometer resolution may be attainable in III–V semiconductors as well.

[1] D. M. Eigler and E. K. Schweizer, Nature **344**, 524 (1990).
[2] J. A. Dagata, J. Schneir, H. H. Harary, C. J. Evans, M. T. Postek, and J. Bennet, Appl. Phys. Lett. **56**, 2001 (1990).
[3] E. S. Snow, P. M. Campbell, and P. J. McMarr, Appl. Phys. Lett. **63**, 749 (1993).
[4] P. M. Campbell, E. S. Snow, and P. J. McMarr, Solid State Electron. **37**, 583 (1994); Appl. Phys. Lett. **66**, 1388 (1995).
[5] S. C. Minne, H. T. Soh, Ph. Flueckiger, and C. F. Quate, Appl. Phys. Lett. **66**, 703 (1995).
[6] J. W. Lyding, T.-C. Shen, J. S. Hubacek, J. R. Tucker, and G. C. Abeln, Appl. Phys. Lett. **64**, 2010 (1994).
[7] E. S. Snow and P. M. Campbell, Appl. Phys. Lett. **64**, 1932 (1994).
[8] W. H. Juan and S. W. Pang, J. Vac. Sci. Technol. B **12**, 422 (1994).
[9] G. C. H. Zau and H. H. Sawin, J. Electrochem. Soc. **139**, 250 (1992).
[10] N. Ozawa, N. Ikegami, Y. Miyakawa, and J. Kanamori, Mater. Res. Soc. Symp. Proc. **236**, 205 (1992).
[11] K. T. Sung and S. W. Pang, J. Vac. Sci. Technol. A **11**, 1206 (1993).
[12] SEM imaging could not accurately resolve the linewidths.
[13] E. S. Snow, P. M. Cambell, and B. V. Shanabrook, Appl. Phys. Lett. **63**, 3488 (1993).